

3D synchrotron laminography assessment of damage evolution in blanked dual phase steels

**Mouhcine Kahziz^{1,2,*}, Thilo Morgeneyer², Matthieu Mazière², Lukas Helfen³,
Eric Maire⁴, Olivier Bouaziz^{1,2}**

¹ ArcelorMittal Research S.A., voie Romaine, F-57239 Maizières-lès-Metz, France

² Mines ParisTech, Centre des Matériaux, UMR CNRS 7633, BP 87, 91003 Evry Cedex, France

³ Institute for Synchrotron Radiation – ANKA, Forschungszentrum Karlsruhe, D-76021 Karlsruhe, Germany

⁴ Université de Lyon, INSA-Lyon, MATEIS CNRS UMR 5510, 20 avenue Albert Einstein, 69621 Villeurbanne, France

* Corresponding author: mouhcine.kahziz@mines-paristech.fr

Abstract

The mechanical performance of automotive structures made of advanced high strength steels (AHSS) is often seen reduced by the presence of cut-edges. Here an attempt is made to gain insight into the initial damage state and the damage evolution during loading of a cut-edge. This is assessed in 3D and in-situ by synchrotron laminography observation during simultaneous tensile and bending loading of a cut-edge produced by stamping. Laminography is a technique that allows to observe regions of interest in thin sheet-like objects. It is found for the DP600 laboratory steel grade that the fracture zone is very rough and that needle voids from the surface and in the material bulk follow ferrite-martensite flow lines. During loading the needle voids grow from the fracture zone surface and coalesce with voids in the bulk. The needle cracks coalesce with the burnish zone through narrow zones, called void sheets. The formed cracks are inclined by 45° compared to the load direction.

Keywords: Dual phase steels, cutting edges, X-ray laminography, damage

1. Introduction

Advanced High Strength Steels (AHSS) grades remain the most widely used and developed materials in the automotive industry in order to reduce the “weight” of structural parts. Among these AHSS grades, dual phase (DP) steels with their ferrite-martensite composite microstructure present a good compromise between strength and formability. DP steels consist of a ferritic matrix containing a hard martensitic second phase in the form of islands. They are produced by controlled cooling from the austenite phase (in hot-rolled products) or from the two-phase ferrite plus austenite phase (for continuously annealed cold-rolled and hot-dip coated products) to transform some austenite to ferrite before a rapid cooling transforms the remaining austenite to martensite. However, the forming processes could affect the mechanical behavior of these grades. Some observations have shown that the cutting step tended to alter the good mechanical properties of this grade [1,2]. These studies have shown that the cutting process of DP sheets affects the adjacent material that extends into the bulk region of the sheet. This affected zone is characterized by a hardening and microstructural deformation which leads to local decohesion of ferritic and martensitic phases [1,11]. This drop in mechanical performance can significantly reduce the properties and then the use of AHSS.

While ductile fracture mechanisms of this steel and its base materials (i.e. ferrite and austenite separately) have been discussed in the past [5,6,7,8], the damage mechanisms of DP cut-edges are not well known. This study aims at offering knowledge of the microstructural initial state of a cut-edge and the evolution of damage from using three dimensions in-situ X-ray synchrotron laminography adapted to 3D observation of regions of interest sheet-like specimen and to identify the damage mechanisms leading to the crack formation initiating from the cut-edge.

X-ray synchrotron laminography has been used in the present study to visualize for the first time

damage evolution from a cut-edge during in-situ tensile bending test. The method, in contrast to computed tomography which is for axisymmetric objects, allows to image in three dimensions a region of interest (for instance the crack tip) inside a sheet-like sample without cutting it. The laminography set-up used here is located at the ID19 beam line at the European Synchrotron Radiation Facility (ESRF) in Grenoble (France). The acquisition was performed with a voxel size of $0.778 \mu\text{m}^3$. Applications in the study of damage of an aluminum grade can be found in the literature [12]. More details about the laminography technique are also given elsewhere [12,13].

2. Material and experiment

2.1. Studied material

The material used in this study is a laboratory dual phase steel with a ultimate tensile strength of approximately 600 MPa and a fracture strain of around 17 % at the as-received condition. The material was supplied as a 0.8mm thick cold rolled sheet. The chemical composition and microstructure are given in figure1.

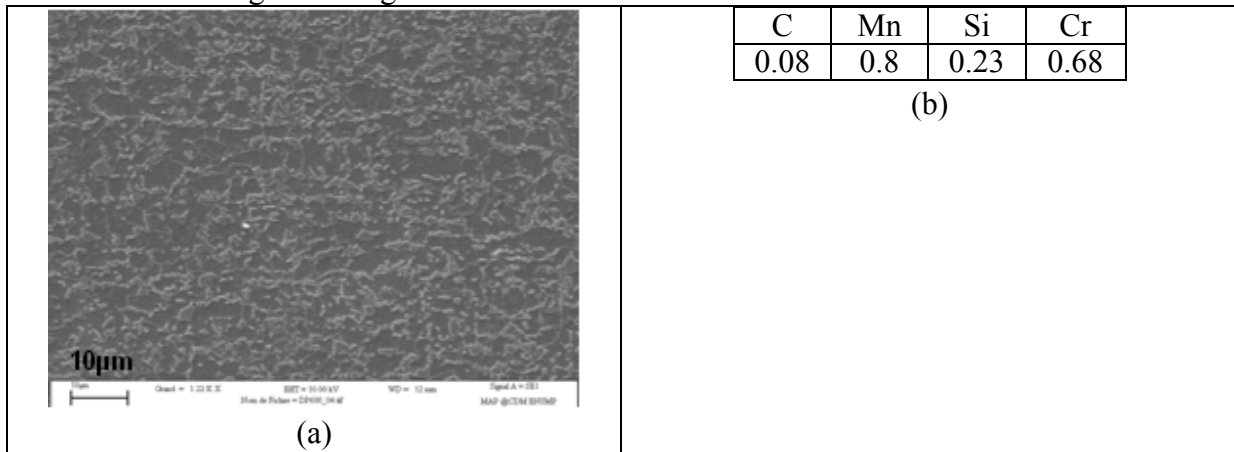


Figure 1: (a) DP microstructure visualized by scanning electron microscopy (after nital 0.2% etching). (b) Chemical composition of DP600 steel (weight %)

The martensite islands appear to be aligned along the rolling direction. In the following the rolling direction will be referred to as L, the long transverse direction as T and the short transverse direction as S.

2.2. The cut-edge profile

The shearing, which is a cutting in a straight line over the entire width of the sheet by the action of a moving blade perpendicular to the plane of the sheet, is the most widely used and least expensive process for separating metal panels. In this study, we assume that the shearing and punching have the same effects on the cut edge as the 2D descriptions of these processes are identical. Figure 2 shows an optical micrograph of the polished surface of a sample after the cutting process. The sheared surface profile is characterized by the existence of 4 characteristic zones: rollover, fracture, burnish and burr (figure2). This observation is consistent with the results found in the literature [1,3].

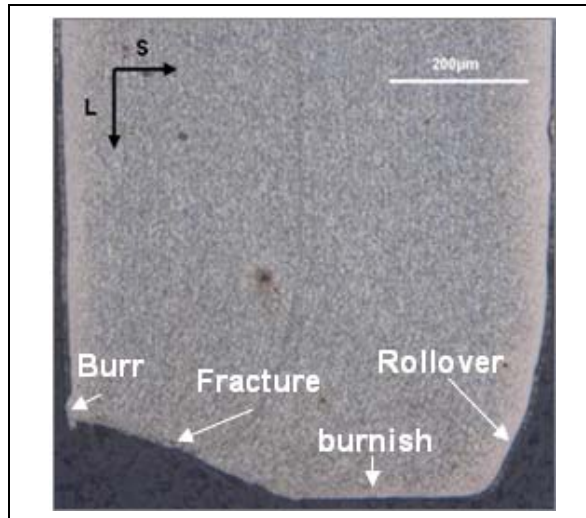


Figure 2: optical micrograph of a DP600 cut-edge profile (after 0.2% nital etching)

The proportion of these 4 characteristic zones are heavily dependent on cutting parameters such as the material nature, clearance, cutting edge radius and cutting speed [3,4,9]. The fracture zone displays the highest damage and presents a high roughness. Some zones of decohesion at the ferrite-martensite interfaces can be observed in the fracture zone and are aligned along the flow lines [1].

2.3. Experiment

The experimental technique used in this study was synchrotron radiation computed laminography (SRCL). It is a non-destructive technique similar to synchrotron radiation computed tomography (SRCT), for three dimensions imaging of objects that are extended in two dimensions. It provides a unique opportunity to observe internal damage mechanisms in three dimensions during extended crack propagation in sheet materials [12]. Unlike SRCT which is especially adapted to compact or one-dimensionally elongated objects which stay in the field of view of the detector system under rotation, SRCL is optimized to image regions of interest (ROIs) out of flat, sheet-like specimens. For this, the specimen rotation axis is inclined at an angle of $\theta < 90^\circ$ with respect to the beam direction ($\theta = 90^\circ$ corresponds to the case of CT). For sheet-like specimens, this enables a relatively constant average X-ray transmission over the entire scanning range of 360° , which allows reliable projection data to be acquired [12]. Although the 3D Fourier domain of the specimen is not sampled completely [13], which leads to imaging artefacts, these artefacts are often less disruptive than the ones produced by (limited-angle) CT [13].

The sample geometry shown in figure3 (a) was used. A hole with a radius of 5 mm was punched out from a sheet of DP steel and an elongated crack was machined up to one edge. The loading was achieved perpendicular to the crack, via a two-screw displacement-controlled wedging device that controls the specimen notch crack mouth opening displacement (CMOD) similar to the one used in Ref. [13,14].

To avoid the sample buckling and out-of-plane motion, an anti-buckling device was used. The entire rig was mounted in a dedicated plate that was removed from the SRCL rotation stage between loading steps. The loading was applied via stepwise increases in the CMOD, one turn of the screw corresponding to 1 mm of CMOD. 3 scans were performed before any loading in order to map and image the initial state of the cut-edge. After each loading step, a scan of the ROI containing the crack tip was carried out.

Observation was performed on the laminography instrument installed at ID19 at the European Synchrotron Radiation Facility (ESRF) in Grenoble (France). The axis inclination angle used was around 30° and a white beam was set up, centered around a 60 keV X-ray energy. The scanned region of interest (ROI) was about 1 mm^3 .

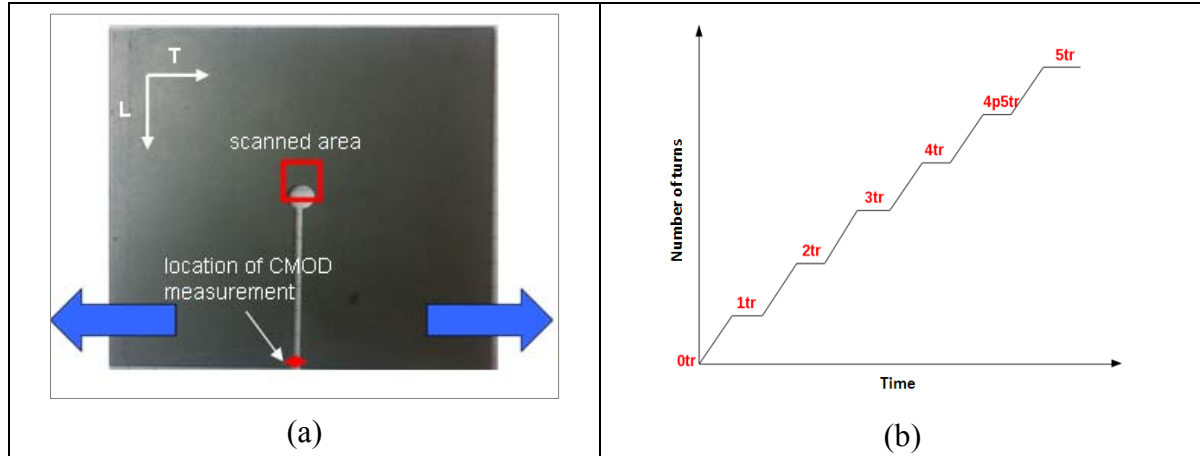


Figure 3: (a) the sample used in in-situ laminography observation and loading direction. (b) Schematic demonstration of stepwise loading applied during the in-situ observation.

3. 2D in-situ visualization of damage evolution from a cut-edge

The figure 4a-f shows the reconstructed 2D laminography sections at different loading stages. Ferrite and martensite phases have the same grayscale due to the fact that the phases have similar attenuation coefficients. They are shown in gray and the initial internal voids can be seen in black in the matrix (ferrite+martensite). Figure 4a shows the material at delivery state after punching in the L-T plane. The 2D sections (figures 4a-f) were taken from the burnish zone. The circular punched hole can be seen at the bottom of the sample. Some artifacts can be observed (cf [12]) that do not influence the segmentation of the voids (figure 5). The 2D sections (figure 4a-f) were taken from the burnish zone. A geometrical defect can be seen in the cut-edge.

Figure 4c, taken from at loading step corresponding to a CMOD equal to 2 mm, shows that a microcrack initiates on the cut-edge close to the geometrical defect. These observations of ductile crack propagation from a cut-edge and coalescence with internal porosities have never been seen before using SRCL with such a high level of details. The coalescence sheets are inclined by 45° compared to the L-direction. Other microcracks initiate from cut-edge but the crack located close to the geometrical defect grows faster. This is consistent with the increased level of stress triaxiality caused by the geometrical defect.

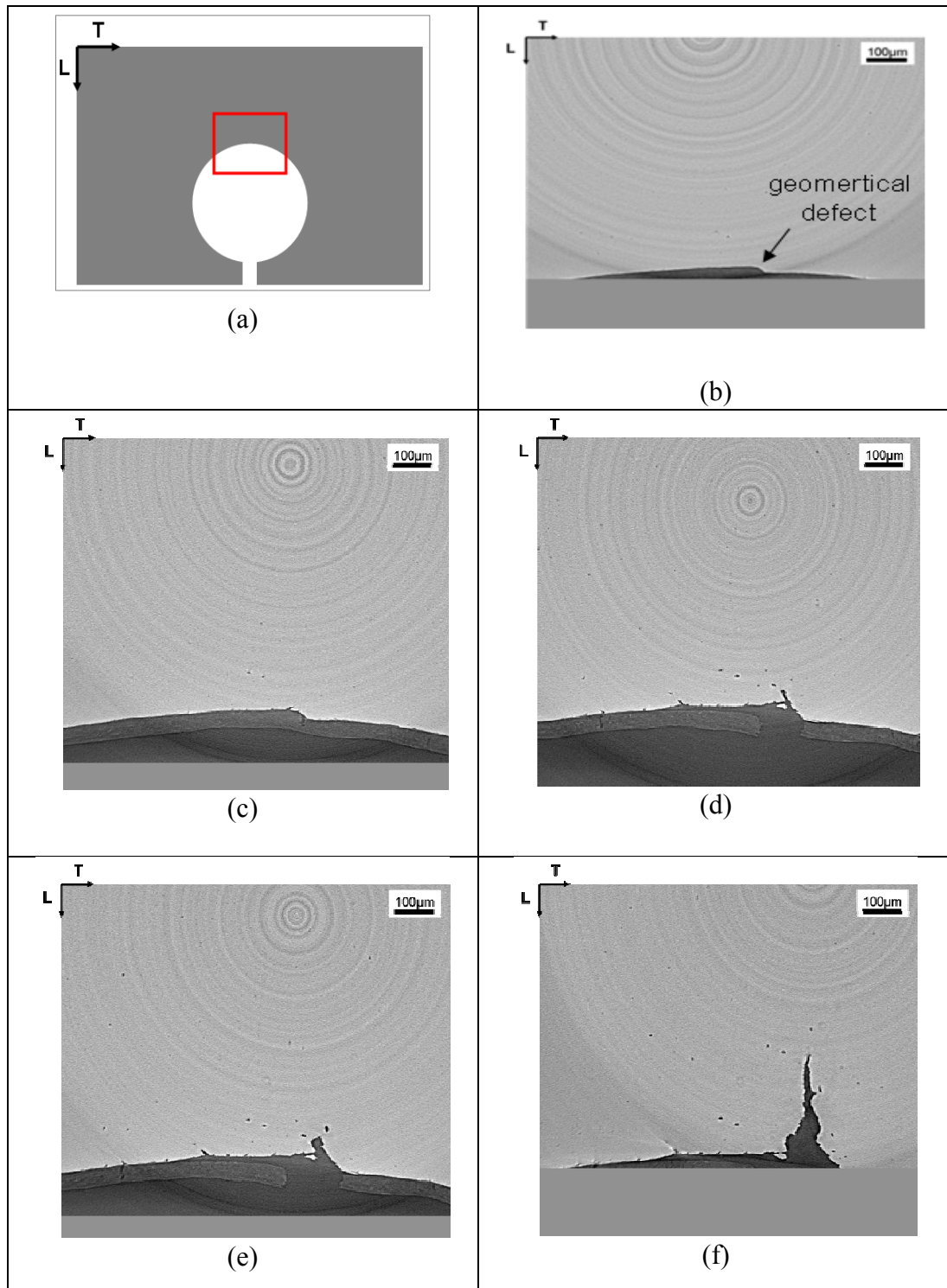


Figure 4: 2D sections at the burnish zone of the steel sheet plane of reconstructed laminography data of damage evolution from a cut-edge at CMODs. (a) The scanned zone (b) material at delivery state; (c) CMOD = 2 mm; (d) CMOD = 3 mm; (e) CMOD = 4 mm; (f) CMOD = 4.5 mm.

4. 3D in-situ observation of damage evolution from a cut-edge

Thanks to SRCL it is possible to visualize the voids in three dimensions, as shown in figure 5a-f, where voids are shown in volumes taken around the mid-thickness at different CMODs. Figure 4a shows the as-received material after punching. The fracture and burnish characteristic zones

surfaces and the geometrical defect located in the fracture-to-burnish transition zone can be seen. The initial porosities can be seen in the bulk of the specimen in black. These voids are aligned along the martensite alignments (interfaces ferrite-martensite) [1]. Coalescence sheets can be seen in figure 5e-f where needle voids growing from the cut-edge, i.e. fracture zone surface, coalesce with the internal needle voids corresponding to the decohesion of ferrite-martensite interfaces. These needle voids then coalesce with the burnish zone through narrow areas known as void sheets.

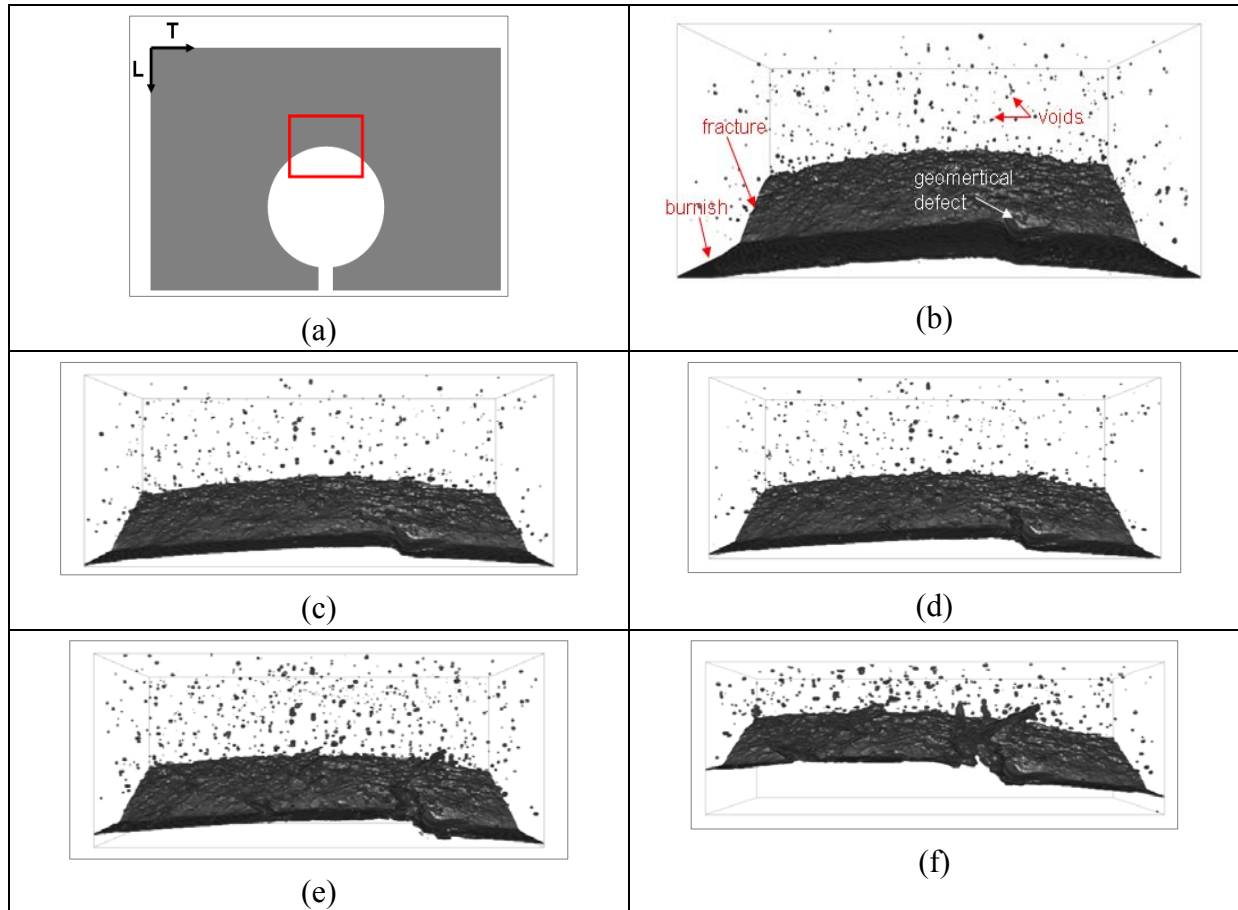


Figure 5: L-T views of 3D volumes of the steel sheet plane of reconstructed laminography data of damage evolution from a cut-edge at CMODs. (a) The scanned zone (b) material at delivery state ($700 \times 350 \times 504 \mu\text{m}^3$); (c) CMOD = 1 mm, ($700 \times 350 \times 294 \mu\text{m}^3$); (d) CMOD = 2 mm, ($700 \times 350 \times 294 \mu\text{m}^3$); (e) CMOD = 3 mm, ($700 \times 350 \times 294 \mu\text{m}^3$); (f) CMOD = 4 mm, ($700 \times 300 \times 260 \mu\text{m}^3$).

Figure 6 shows the shape of needle voids grown from the fracture zone surface and in the bulk. These needle voids consist with the decohesion of ferrite-martensite interfaces (i.e. the flow lines) characterized in Ref [1].

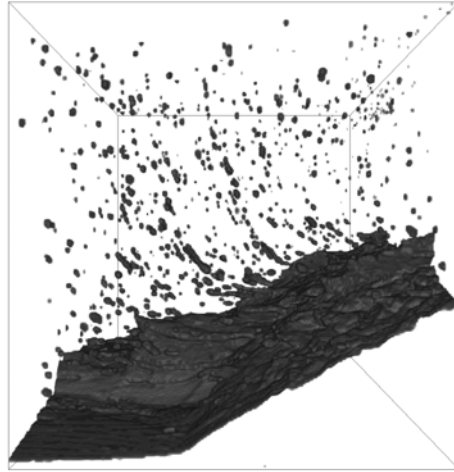


Figure 6: L-S 3D view of reconstructed laminography data of a DP600 cut-edge at CMOD = 3 mm (260x350x700 μm^3)

Figure 7 shows L-S views of reconstructed laminography data of DP600 cut-edge. Figure 7a illustrates the cut-edge profile with the 4 characteristic zones. Microcracks, needle voids from the fracture zone surface and needle voids in the bulk can be seen in figure 7a. Figure 7b shows the coalescence sheet of needle voids growing from the fracture zone and the burnish zone.

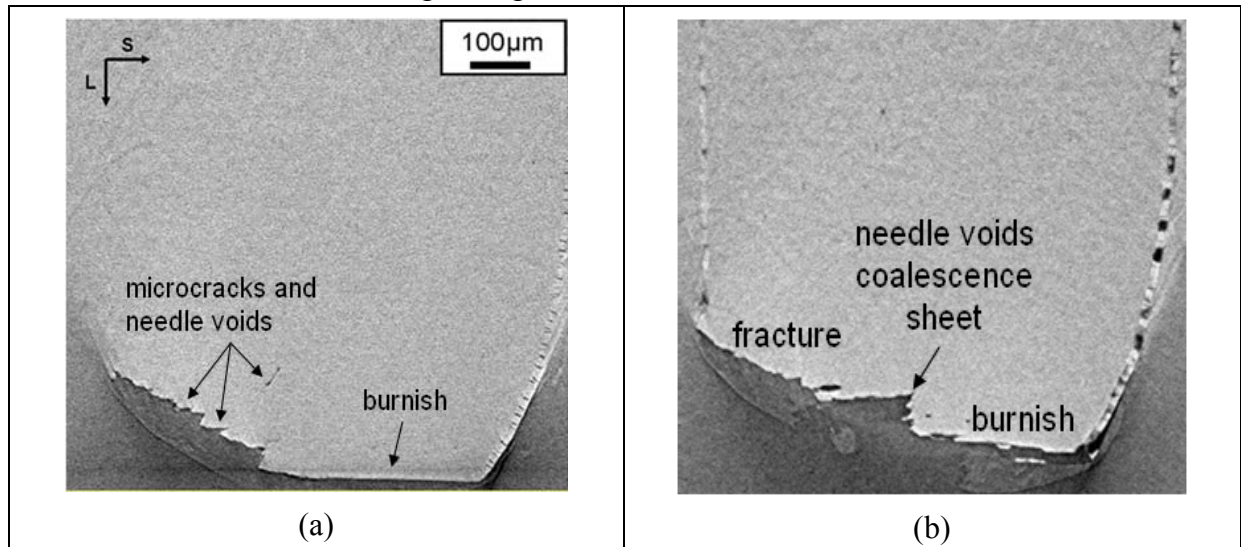


Figure 7: L-S 2D sections of reconstructed laminography data. (a) cut-edge profile at initial state. (b) Coalescence sheet at CMOD = 3 mm.

5. Conclusion

The experimental study presented in this paper aims at gaining insight into the initial damage state and subsequent damage evolution during mechanical loading from DP600 steel grade cut-edges. 3D imaging using synchrotron radiation computed laminography has allowed us to identify different defects that a cut-edge at initial state contains. These include roughness in the fracture zone, needle voids in the bulk from fracture zone and alignment of needle voids along the flow lines i.e. martensite alignments. These results are consistent with the ones found in Ref. [1,3].

The 3D in-situ laminography observation, particularly adapted to the observation of sheet-like objects, carried out on a sample with a circular punched hole has allowed us to characterize, for the first time, the damage evolution from a cut-edge in-situ and in 3D during mechanical tension and bending loading. The growth of needle voids was especially along flow lines from fracture zone surface but also in the bulk along the martensite alignments. The initial void growth direction is parallel to the burnish plan and normal to the loading direction. We observe that the coalescence of needle voids from the fracture zone with the burnish zone occurs via narrow coalescence zones. These cracks are inclined by 45° compared to the L-direction. Several cracks are formed, especially in the fracture zone, but the one located close to the geometrical defect grows faster. This is consistent with the increased level of stress triaxiality that is known to favor ductile damage growth.

References

- [1]: A. Dalloz, J. Besson, A.-F. Gourgues-Lorenzon, T. Sturel, A. Pineau, Effect of shear cutting on ductility of a dual phase steel, *Engineering Fracture Mechanics*, 76 (2009) 1411 – 1424.
- [2]: Daniel J. Thomas, Effect of Mechanical Cut-Edges on the Fatigue and Formability Performance of Advanced High-Strength Steels, *Failure Analysis and Prevention*, 12 (2012) 518-531.
- [3]: X. Wu, H. Bahmanpour, K. Schmid, Characterization of mechanically sheared edges of dual phase steels, *Materials Processing Technology*, 212 (2012) 1209 – 1224.
- [4]: H. So, D. Fasmann, H. Hoffmann, R. Golle, M. Schaper, An investigation of the blanking process of the quenchable boron alloyed steel 22MnB5 before and after hot stamping process, *Materials Processing Technology*, 212 (2012) 437-449.
- [5]: C. Landron, O. Bouaziz, E. Maire, J. Adrien, Characterization and modeling of void nucleation by interface decohesion in dual phase steels, *Scripta Materialia*, 63 (2010) 973–976.
- [6]: C. Landron, E. Maire, O. Bouaziz, J. Adrien, L. Lecarme, A. Bareggi, Validation of void growth models using X-ray microtomography characterization of damage in dual phase steels, *Acta Materialia*, 59 (2011) 7564–7573.
- [7]: X. Sun and K.S. Choi and A. Souلامي and W.N. Liu and M.A. Khaleel, On key factors influencing ductile fractures of dual phase (DP) steels, *Materials Science and Engineering*, 526 (2009) 140 – 149.
- [8]: M. Ben Bettaieb, X. Lemoine, O. Bouaziz, A. M. Habraken and L. Duchane, Numerical modeling of damage evolution of DP steels on the basis of X-ray tomography measurements, *Mechanics of Materials*, 43 (2011) 139 – 156.
- [9]: B.S. Levy and C.J. Van Tyne, Review of the Shearing Process for Sheet Steels and Its Effect on Sheared-Edge Stretching, *Material and Engineering Performance*, (2011) 1-9.
- [10]: B.S. Levy and C.J. Van Tyne, Effect of a Strain-Hardening Rate at Uniform Elongation on Sheared Edge Stretching, *Materials Engineering and Performance*, (2012) 1-8.
- [11]: M. Azuma, S. Goutianos, N. Hansen, G. Winther and X. Huang, Effect of hardness of martensite and ferrite on void formation in dual phase steel, *Materials Science and Technology*, 28 (2012) 1092-1100.
- [12]: T.F. Morgeneyer, L. Helfen, I. Sinclair, H. Proudhon, F. Xu and T. Baumbach, Ductile crack initiation and propagation assessed via in situ synchrotron radiation-computed laminography, *Scripta Materialia*, 65 (2011), 1010–1013.
- [13]: L. Helfen, T. Baumbach, P. Mikulik, D. Kiel, P. Pernot, P. Cloetens, J. Baruchel, High-resolution three-dimensional imaging of flat objects by synchrotron-radiation computed laminography, *Applied Physics Letters*, 86 (2005) 071915.
- [14]: L. Helfen, A. Myagotin, P. Mikulik, P. Pernot, A. Voropaev, M. Elyyan, M. Di Michiel, J. Baruchel, and T. Baumbach, On the implementation of computed laminography using synchrotron radiation, *Review of Scientific Instruments*, 82 (2011) 063702.